

On the Role of Large-Scale Transient Eddies in the Maintenance of the Vorticity and Enstrophy of the Time-Mean Atmospheric Flow

E. O. HOLOPAINEN¹

Geophysical Fluid Dynamics Program, Princeton University, Princeton, NJ 08540

A. H. OORT

Geophysical Fluid Dynamics Laboratory/NOAA, Princeton University, Princeton, NJ 08540

(Manuscript received 30 June 1980, in final form 21 October 1980)

ABSTRACT

The global distribution of the forcing of the time-mean flow due to large-scale, horizontal Reynolds stresses ($\overline{u'u'}$, $\overline{v'v'}$, $\overline{u'v'}$) is determined from upper wind statistics for the period 1968–73. The role of this forcing in the maintenance of the vorticity and enstrophy of the time-mean flow is discussed.

The most striking effect of transient eddy stresses is the tendency to shift the subtropical maxima in the time-mean flow and the associated vorticity patterns poleward. However, significant longitudinal variations in forcing occur, also. Calculations of the dominant terms in vorticity budgets of the North Pacific Low, the North Atlantic Low, and the Siberian High, which may be called the centers of action of winter-time circulation at sea level in the Northern Hemisphere, are presented. In all three cases, transient eddies are found to be important in maintaining the centers against the dissipative action of surface friction.

In terms of the enstrophy budget, the hemispheric and global-mean effects of transient eddies on the mean flow are small, both in December–February and June–August. In the Northern Hemisphere, where the results are most reliable, the eddies are weakly dissipative with a time scale on the order of several months.

When separating the time-mean flow into the contributions from the axisymmetric component and from the stationary disturbances, it is found that the transient eddy stresses tend to maintain the axisymmetric mean flow, but to weaken the stationary disturbances. There are significant latitudinal variations in the enstrophy forcing of the stationary disturbances. Thus eddy forcing is an important factor in maintaining the enstrophy of stationary disturbances in the extratropics, while it tends to destroy their enstrophy in the tropics.

1. Introduction

The influence of large-scale synoptic eddies on the time-mean flow is one of the most difficult effects to include in climate models. This forcing has two aspects, one related to heat transport, the other to momentum transport. All climate models constructed so far take in some way the eddy heat transport into account, which is often tacitly assumed to be the primary factor.

In a recent paper Holopainen (1978, hereafter referred to as H) has given empirical evidence that the momentum transport by transient eddies also is important for the maintenance of the time-averaged flow. In H most emphasis was put on annual-mean conditions. More recently, Lau (1979) has calculated the contributions of both the time-mean flow and transient eddies to the local balances of heat and

vorticity in the Northern Hemisphere north of 20°N in winter. His results suggest that the effects of transient disturbances are considerably smaller than those of the mean flow. Lau found this to be the case both for the heat and the vorticity budgets.

In order to further clarify the role of the transient eddies in maintaining the time-mean flow, global upper air statistics for the period May 1968–April 1973 are used here to study certain aspects of the atmospheric vorticity budget for December–February and June–August. The global analyses used are part of a 15-year data set compiled at the Geophysical Fluid Dynamics Laboratory, Princeton.² The network of aerological stations, from which the basic observations were obtained, is shown in Fig. 1. The method of deriving horizontal analyses for the various statistical quantities is similar to the one described by Oort and Rasmusson (1971).

¹ On leave from the Department of Meteorology, University of Helsinki, Helsinki, Finland.

² Oort, A. H., 1981: Global atmospheric circulation statistics, 1958–1973. NOAA Prof. Pap. (in preparation).

DISTRIBUTION WIND REPORTING STATIONS FOR JAN 71 AT 300mb (N_{GLOBE} = 735)

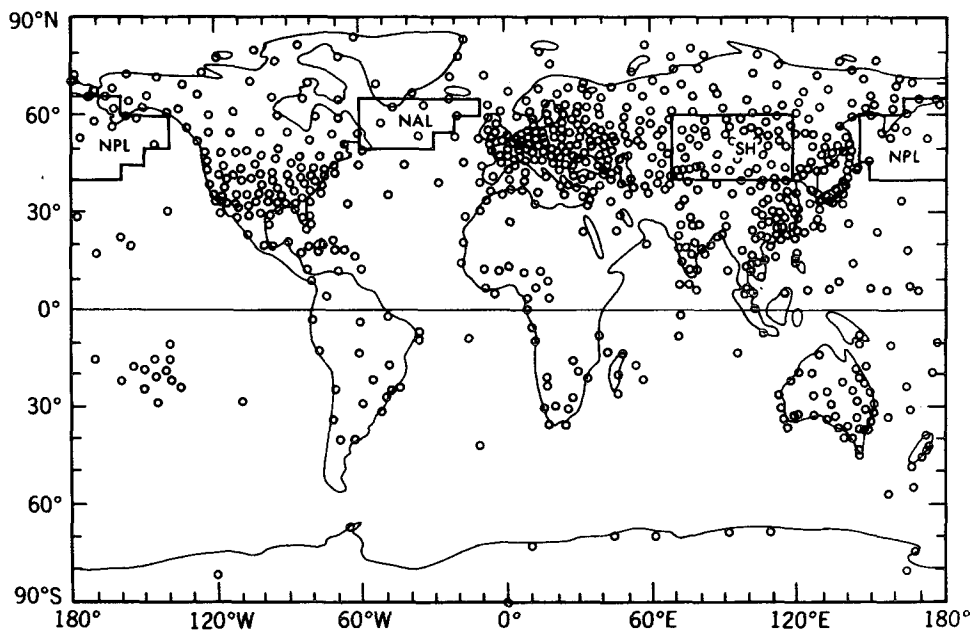


FIG. 1. Distribution of the rawinsonde stations at 300 mb from which the basic observations for the GFDL data set were obtained for a typical month (January 1971). Also shown are the areas of the North Pacific low (NPL), North Atlantic low (NAL) and Siberian high (SH).

2. Vorticity-forcing of the time-mean atmospheric flow by large-scale transient eddies

a. Equations

It was shown in H that the vorticity equation for the time-mean flow can be written as

$$\frac{\partial \bar{\zeta}}{\partial t} = -\bar{\mathbf{V}} \cdot \nabla \bar{\eta} + \text{curl } \mathbf{A}_H + f \frac{\partial \bar{\omega}}{\partial p} + \text{curl } \bar{\mathbf{F}} + \bar{\zeta} \frac{\partial \bar{\omega}}{\partial p} - \bar{\omega} \frac{\partial \bar{\zeta}}{\partial p} - \mathbf{k} \cdot \nabla \bar{\omega} \times \frac{\partial \bar{\mathbf{V}}}{\partial p} + \text{curl } \mathbf{A}_V, \quad (1)$$

where, as usual, the bar denotes a time-average and a prime a deviation from it. Further $\mathbf{V} (=u\mathbf{i} + v\mathbf{j})$ = the horizontal wind, $\omega = dp/dt$, $\zeta = \mathbf{k} \cdot \nabla \times \mathbf{V}$, $\eta = f + \zeta$, f = Coriolis parameter, and $\text{curl } \mathbf{B} = \mathbf{k} \cdot \nabla \times \mathbf{B}$, where \mathbf{B} is an arbitrary vector. \mathbf{F} is the frictional force due to small-scale turbulence, whereas $\mathbf{A} = \mathbf{A}_H + \mathbf{A}_V$ is the horizontal force due to the presence of large-scale transient eddies, where

$$\mathbf{A}_H = A_\lambda \mathbf{i} + A_\phi \mathbf{j}, \quad (2)$$

$$A_\lambda = -\frac{1}{a \cos \phi} \frac{\partial}{\partial \lambda} \overline{u'u'} - \frac{1}{a \cos \phi} \frac{\partial}{\partial \phi} \overline{u'v'} \cos \phi + \frac{\overline{u'v'}}{a} \tan \phi, \quad (3)$$

$$A_\phi = -\frac{1}{a \cos \phi} \frac{\partial}{\partial \lambda} \overline{u'v'} - \frac{1}{a \cos \phi} \frac{\partial}{\partial \phi} \overline{v'v'} \cos \phi - \frac{\overline{u'u'}}{a} \tan \phi, \quad (4)$$

$$A_V = -\frac{\partial}{\partial p} \overline{\mathbf{V}'\omega'}. \quad (5)$$

The vorticity forcing of the time-mean flow by the transient eddies is, according to (1), given by $\text{curl } \mathbf{A}_H + \text{curl } \mathbf{A}_V$. Having statistics of $\overline{u'u'}$, $\overline{u'v'}$ and $\overline{v'v'}$ at our disposal, Eqs. (3) and (4) enable us to determine the patterns of \mathbf{A}_H , and thus also of $\text{curl } \mathbf{A}_H$. However, $\text{curl } \mathbf{A}_V$ cannot be calculated from the present data. In his diagnostic calculations based on routine objective analyses by the National Meteorological Center (NMC), Lau (1979) used daily vertical velocities from the operational forecast model to derive patterns of $\overline{u'\omega'}$ and $\overline{v'\omega'}$ for the Northern Hemisphere in winter. Lau's results (personal communication) indicate that $\text{curl } \mathbf{A}_V$ is typically one order of magnitude smaller than $\text{curl } \mathbf{A}_H$. Furthermore, if the vertically-averaged (barotropic) flow is considered, $\text{curl } \mathbf{A}_V$ is identically zero. With these facts in mind, we will assume that $\text{curl } \mathbf{A}_H$ represents the total forcing of the time-mean flow due to transient eddies.

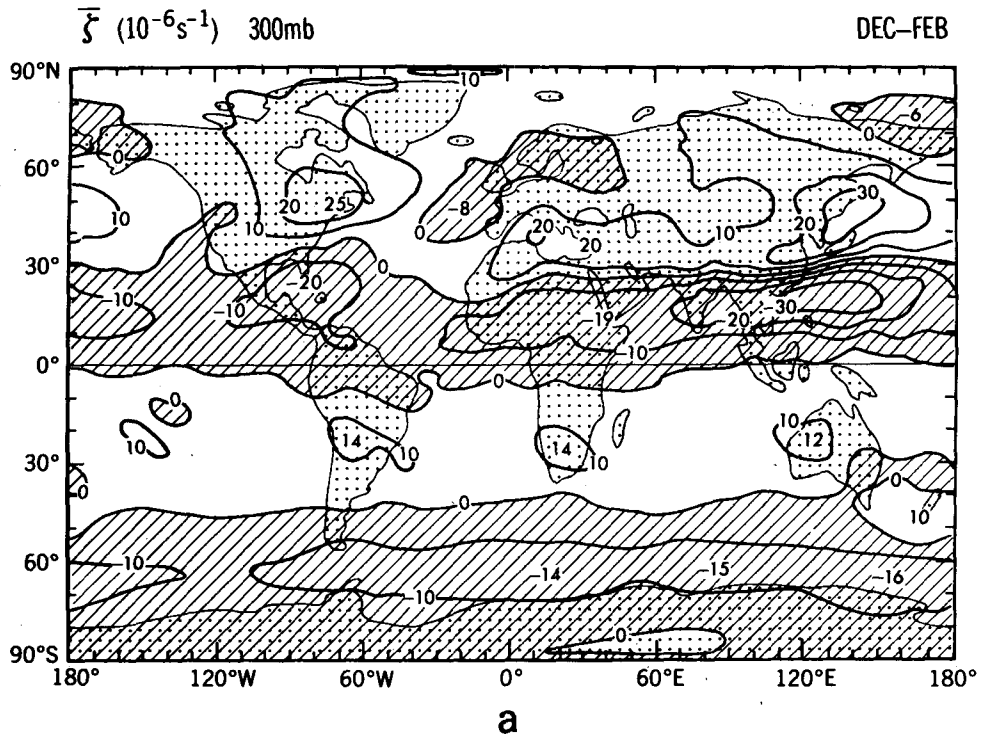


FIG. 2a. Mean vorticity $\bar{\zeta}$ ($10^{-6} s^{-1}$) at 300 mb for December-February.

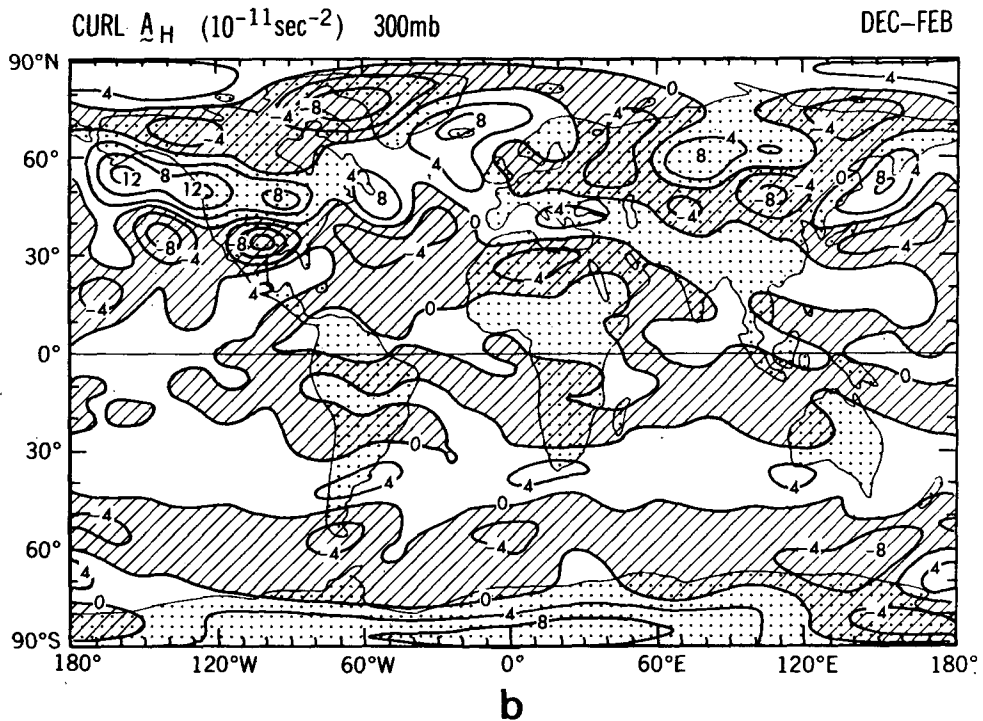


FIG. 2b. Transient eddy vorticity forcing curl A_H ($10^{-11} s^{-2}$) at 300 mb for December-February.

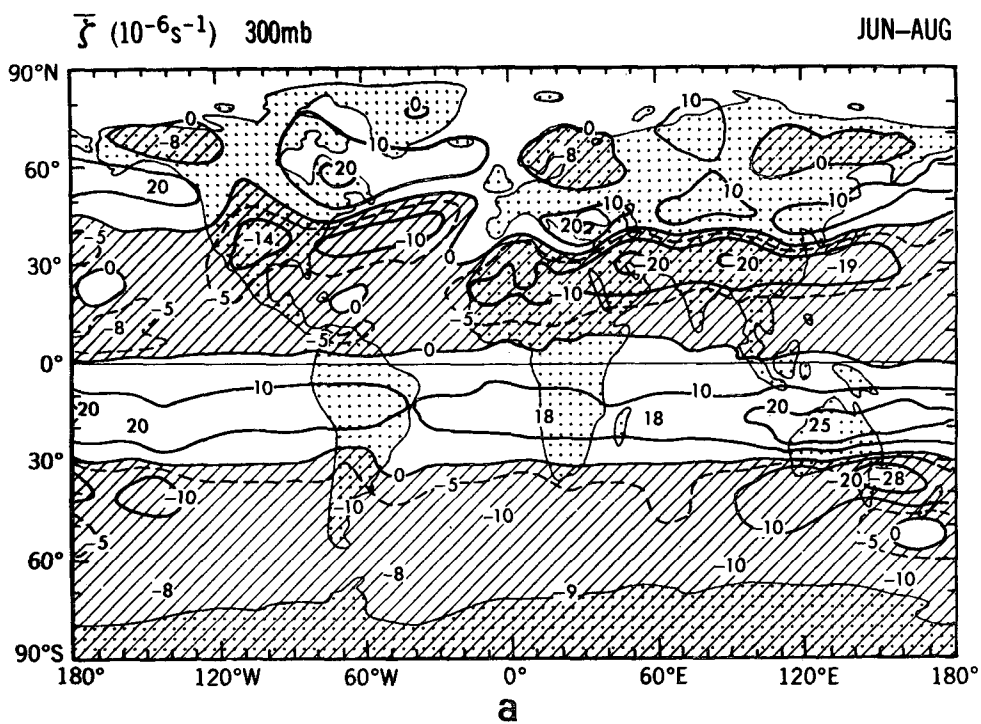


FIG. 3a. Mean vorticity $\bar{\zeta}$ (10^{-6} s^{-1}) at 300 mb for June–August.

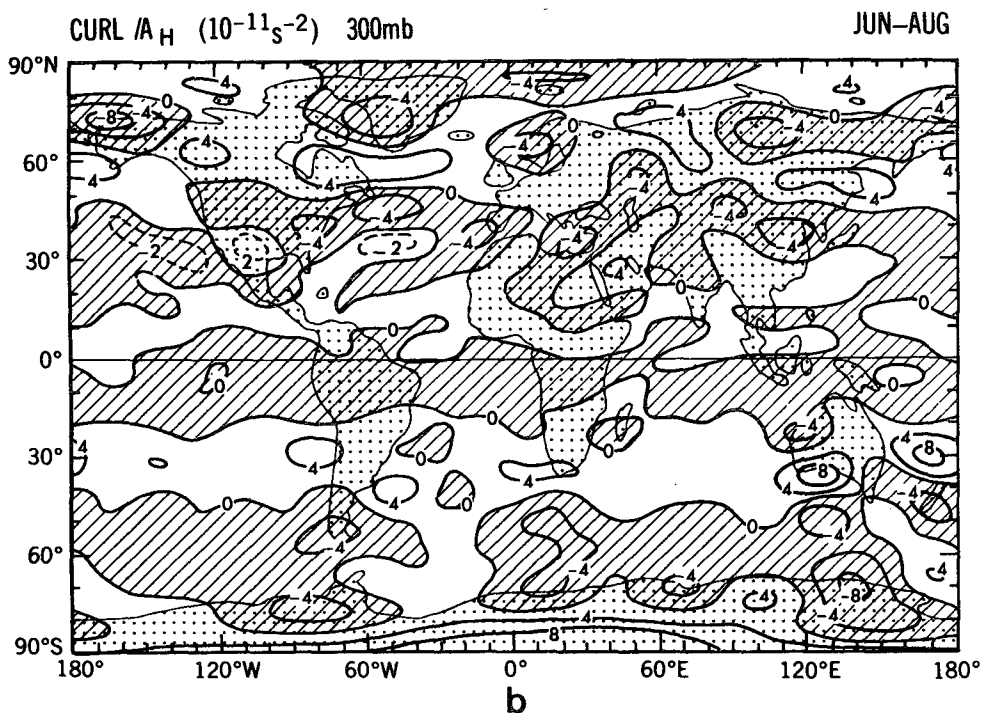


FIG. 3b. Transient eddy vorticity forcing curl A_H (10^{-11} s^{-2}) at 300 mb for June–August.

TABLE 1. Standard deviations (10^{-11} s^{-2}) of curl A_H and $-\bar{V} \cdot \nabla \bar{\eta}$ along various latitude circles at 300, 500 and 700 mb during December–February.

Height (mb)	Latitude								
	0°	10°	20°	30°	40°	50°	60°	70°	80°N
300									
curl A_H	0.6	1.5	3.0	3.9	4.7	6.7	5.1	6.2	5.8
$\bar{V} \cdot \nabla \bar{\eta}$	1.1	2.6	5.6	10.6	11.7	7.1	3.4	4.0	2.4
500									
curl A_H	0.3	0.6	1.2	2.1	2.3	3.0	3.5	4.2	4.5
$\bar{V} \cdot \nabla \bar{\eta}$	0.8	1.3	2.7	4.9	4.5	4.2	3.0	2.3	1.7
700									
curl A_H	0.5	0.5	1.0	1.8	1.9	1.9	2.9	2.7	3.5
$\bar{V} \cdot \nabla \bar{\eta}$	1.4	1.7	1.5	2.5	3.0	3.0	2.5	1.4	1.2

b. Global and hemispheric features

The geographical distributions of $\bar{\zeta}$ and curl A_H are shown in Figs. 2 and 3 at the 300 mb level for December–February and June–August, respectively. At this level, most velocity-related quantities reach their maximum amplitude. (The patterns of curl A_H in Figs. 2b and 3b are smoothed fields obtained by making a spherical harmonic analysis of the original fields, and retaining only those components P_n^m for which the zonal wavenumber $m \leq 10$ and $n \leq 20$.) The figures show clearly that the time-mean circulation is more axisymmetric in the Southern than in the Northern Hemisphere. The three “dipoles” in the Northern Hemisphere $\bar{\zeta}$ field in winter are associated with the well-known jet stream maxima of the time-mean flow.

The forcing due to transient eddies, curl A_H , also has a strong axisymmetric component with anticyclonic forcing centered at a latitude of about 30° in winter and 40° in summer, whereas cyclonic forcing is found more poleward until a latitude of $\sim 70^\circ$. However, longitudinal variations do occur as was already shown by Lau (1979; see his Fig. 8) for the winter case. One measure of the amplitude of these variations is the standard deviation along a latitude circle. The standard deviations of curl A_H and $\bar{V} \cdot \nabla \bar{\eta}$ are given in Table 1 for the Northern Hemisphere in winter. It is found that south of 50°N the magnitude of $\bar{V} \cdot \nabla \bar{\eta}$ is two to three times larger than that of curl A_H , which roughly agrees with Lau's (1979) findings. However, north of 50°N the variations in transient forcing dominate. As we will see in Section 2c, the term $\bar{V} \cdot \nabla \bar{\eta}$ tends to have a different sign in the lower and upper troposphere, whereas the profile of curl A_H does not change sign in the vertical. This makes the transient forcing particularly important for the vertically-averaged (barotropic) mean flow.

Figs. 4a and 4b show meridional profiles of the zonally and vertically averaged $\bar{\zeta}$ and curl A_H (in the figure brackets denote a zonal average, and carets a

vertical average over the layer 50–1000 mb). The distributions at any particular pressure level are qualitatively similar to the integrated ones shown in Fig. 4. However, the magnitudes of both $\bar{\zeta}$ and curl A_H are smaller in the lower troposphere, and larger above 500 mb than the vertical average. It is obvious from Fig. 4 that one important effect of the transient eddies is the tendency to shift the subtropical maximum of the mean westerly wind and the associated vorticity distribution poleward. [In terms of the momentum budget this means that the strongest eddy convergence of zonal momentum ($\partial[\bar{u}'v']/\partial y < 0$) takes place somewhat poleward of the subtropical jetstream.] In middle latitudes the forcing of the zonally averaged time-mean flow is seen to be roughly in phase with the vorticity itself thus tending to reinforce the vorticity pattern.

c. Vorticity budget for the wintertime “centers of action” in the Northern Hemisphere

It is of some interest to consider the vorticity budget in certain climatologically significant areas. The most striking features of the wintertime mean circulation at sea level in the Northern Hemisphere are the North Pacific Low, the North Atlantic Low and the Siberian High. Their domain, shown schematically in Fig. 1, is here defined roughly as the area within the 1012, 1008 and 1030 mb isobars, respectively. The North Pacific and Atlantic lows are obviously sink regions, while the Siberian high is a source region for atmospheric vorticity. The question arises how these quasi-permanent features are maintained.

Fig. 5 shows the vertical distribution of $-\bar{V} \cdot \nabla \bar{\eta}$ and curl A_H for these centers of action. Considering first the North Pacific low, we find that the term $-\bar{V} \cdot \nabla \bar{\eta}$ changes sign in the vertical. Thus it tends to increase the local vorticity in the upper troposphere, and to decrease the vorticity in the lower troposphere. At any particular level the term $-\bar{V} \cdot \nabla \bar{\eta}$ has a smaller magnitude than its components $-\bar{V} \cdot \nabla \bar{\zeta}$ and $-\beta \bar{v}$, since they tend to counteract each other (not shown). The term curl A_H , is positive (i.e., cyclonic forcing) throughout the troposphere and its magnitude is comparable with that of $-\bar{V} \cdot \nabla \bar{\eta}$.

Integration of (1) over the mass of the entire air column gives over a level surface (see H or Holopainen and Oort, 1981) the approximate relation

$$\text{curl } \bar{\tau}_s = - \int_0^{\bar{p}_s} \bar{V} \cdot \nabla \bar{\eta} \frac{dp}{g} + \int_0^{\bar{p}_s} \text{curl } A_H \frac{dp}{g}, \quad (6)$$

where $\bar{\tau}_s$ denotes the stress of the atmosphere on the underlying surface and \bar{p}_s the mean surface pressure.

The sum of the vertically integrated values of $-\bar{V} \cdot \nabla \bar{\eta}$ and curl A_H therefore can be compared with independent estimates of curl $\bar{\tau}_s$ computed from sur-

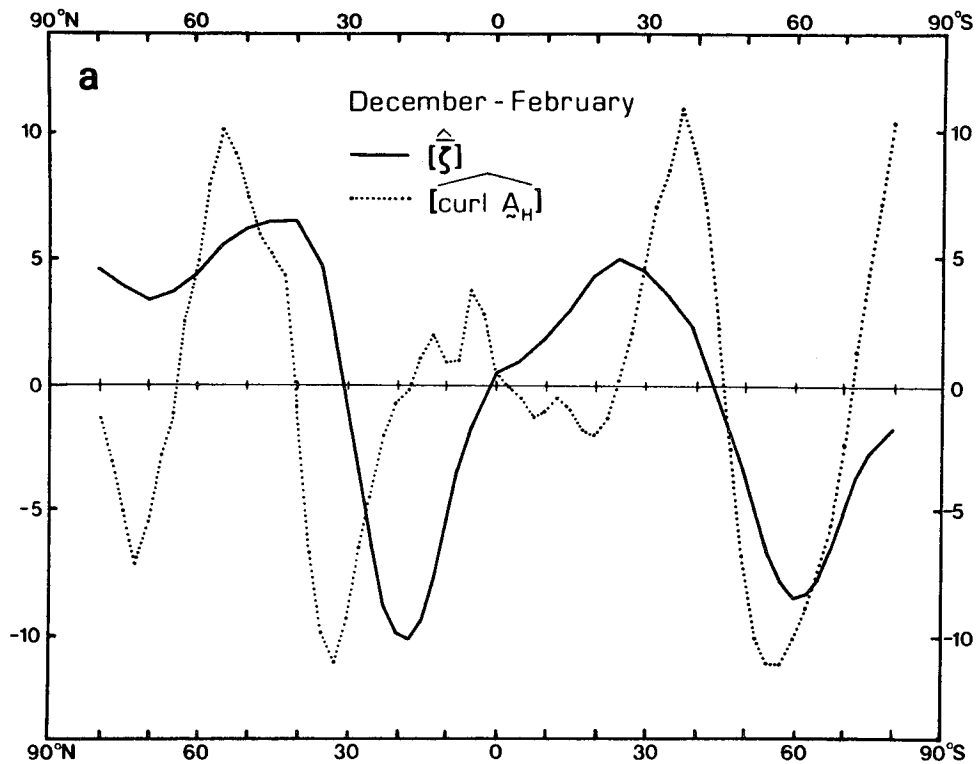


FIG. 4a. Meridional profiles of ζ (solid line) and $\text{curl } A_H$ (dashed line), averaged with respect to longitude and pressure, for December-February. Units for ζ 10^{-6} s^{-1} ; for $\text{curl } A_H$ 10^{-12} s^{-2} .

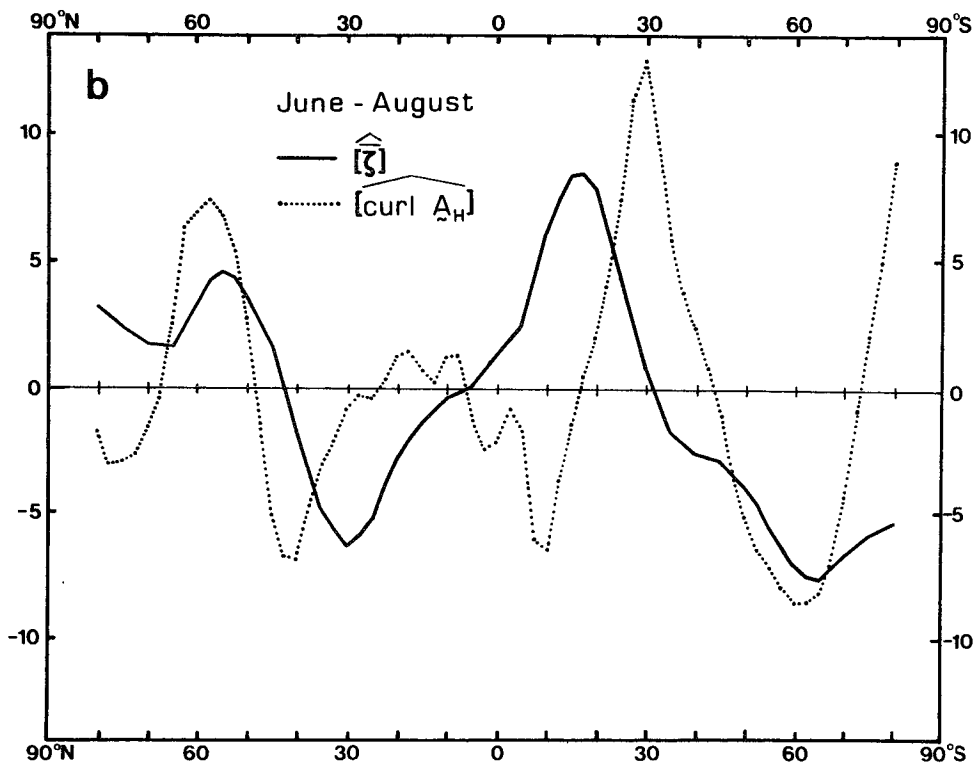


FIG. 4b. As in Fig. 4a but for June-August.

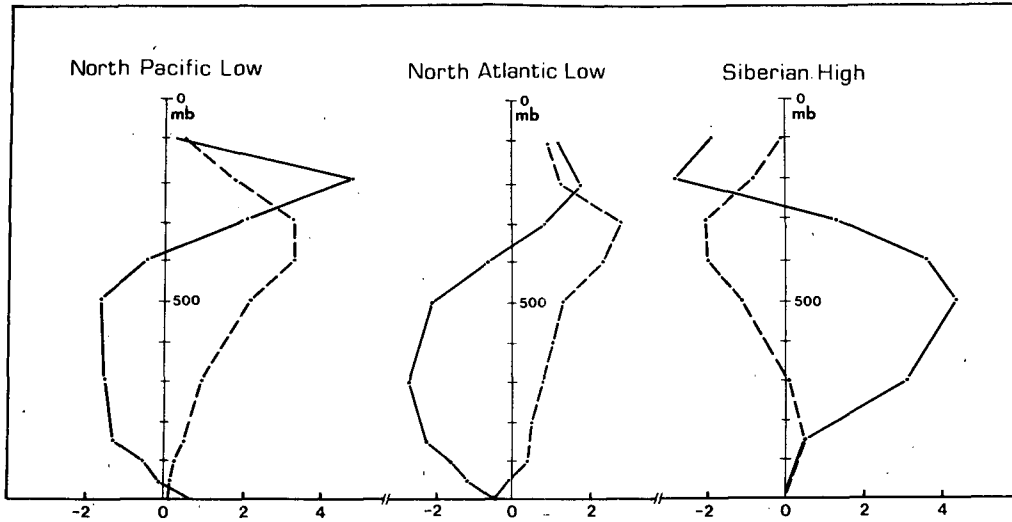


FIG. 5. Vertical profiles of $-\bar{\mathbf{V}} \cdot \nabla \bar{\eta}$ (solid line) and $\text{curl } \mathbf{A}_H$ (dashed line) for the North Pacific low, the North Atlantic low and the Siberian high during December–February (units: 10^{-11} s^{-2}).

face data using a drag-law formulation. Such surface computations of $\text{curl } \bar{\tau}_s$ were kindly provided to us by Sol Hellerman (personal communication). The results for the various terms in case of the North Pacific low are

$$M = - \int_{50}^{1000} \bar{\mathbf{V}} \cdot \nabla \bar{\eta} \frac{dp}{g} = -0.2 \times 10^{-7} \text{ N m}^{-3},$$

$$T = \int_{50}^{1000} \text{curl } \mathbf{A}_H \frac{dp}{g} = 1.5 \times 10^{-7} \text{ N m}^{-3},$$

$$\text{curl } \bar{\tau}_s \text{ (sfc data)} = 0.9 \times 10^{-7} \text{ N m}^{-3}.$$

Considering the uncertainties, especially in the estimate of M (see Holopainen and Oort, 1981), the agreement between $M + T$ and $\text{curl } \bar{\tau}_s$ (sfc data) above is fairly good. Our main conclusion is that in the North Pacific low transient disturbances are the dominant mechanism for bringing in cyclonic vorticity from outside the region to compensate for the frictional sink at the surface.

The results for the North Atlantic low are qualitatively similar. The estimate of $\text{curl } \bar{\tau}_s$ (sfc data) for this region based on Hellerman's wind-stress data is $1.8 \times 10^{-7} \text{ N m}^{-3}$. Large-scale atmospheric turbulence again brings in vorticity from the atmosphere outside at a rate of $T = 1.1 \times 10^{-7} \text{ N m}^{-3}$. The term M as evaluated from our data turns out to be negative ($-0.8 \times 10^{-7} \text{ N m}^{-3}$), but the error limits for this estimate are so large that even its sign is uncertain. In any case, the role of transient atmospheric disturbances in the maintenance of the vorticity budget of the North Atlantic low is the same as that for the North Pacific low.

The vertical profile of the vorticity budget for the Siberian high, as shown in Fig. 5, is the reverse of

that for the lows. This continental, high-pressure region is obviously a source of atmospheric vorticity ($\text{curl } \bar{\tau}_s < 0$). Unfortunately, no independent estimate of its strength can be made from surface data, as was the case over the oceans. An important point to notice is that transient disturbances again provide a mechanism for the horizontal vorticity transport, in this case away from the source region.

Estimates of the horizontal divergence based directly on observed winds are not reliable enough to allow a detailed investigation of the vorticity budget at different pressure levels. However, as a first approximation one can assume (as in H) that the vorticity balance in the free atmosphere is given by $f \nabla \cdot \bar{\mathbf{V}} \approx -\bar{\mathbf{V}} \cdot \nabla \bar{\eta} + \text{curl } \mathbf{A}_H$, and, in the atmospheric boundary layer, by $f \nabla \cdot \bar{\mathbf{V}} \approx -g(\partial/\partial p) \text{curl } \tau$. In light of these equations, the results shown in Fig. 5 for $-\bar{\mathbf{V}} \cdot \nabla \bar{\eta}$ and $\text{curl } \mathbf{A}_H$ imply that there is mean ascending motion in both lows and descending motion in the Siberian high. Furthermore, both the mean-flow term ($-\bar{\mathbf{V}} \cdot \nabla \bar{\eta}$) and the transient eddy term ($\text{curl } \mathbf{A}_H$) are important for these mean vertical velocities. Because the magnitude of the total advection, $-\bar{\mathbf{V}} \cdot \nabla \bar{\eta} + \text{curl } \mathbf{A}_H$, is largest in the upper troposphere and the frictional source or sink is at the surface, the mean vertical velocities must be important in providing the necessary exchange of vorticity between the upper troposphere and the surface boundary layer.

3. The effects of large-scale transient eddies on the entrophy balance of the time-mean flow.

To obtain a global or hemispheric measure of the effects of large-scale turbulence on the time-mean flow, vorticity itself is not a good quantity to study

TABLE 2. Enstrophy S , rate of change of enstrophy due to the transient eddy forcing $(\partial S/\partial t)_T$, and corresponding time scales (negative for dissipative effects) for the time-mean flow, the zonally averaged time-mean flow and the stationary disturbances averaged over the Northern Hemisphere (NH), the Southern Hemisphere (SH) and the globe (GL). All numbers refer to vertical averages between 50 and 1000 mb. For definition of the symbols, see Eqs. (7)–(13). Units for S_M, S_{MZ} and S_{ME} : 10^{-12} s^{-2} ; for their rate of change: 10^{-17} s^{-3} ; and for the time scales: days.

		December–February			June–August		
		NH	SH	GL	NH	SH	GL
Time-mean flow	S_M	38	13	26	15	25	20
	$\left(\frac{\partial S_M}{\partial t}\right)_T$	0.08	1.40	0.74	0.26	0.06	0.17
	$S_M \left(\frac{\partial S_M}{\partial t}\right)_T^{-1}$	>60	12	41	>60	>60	>60
Zonally averaged time-mean flow	S_{MZ}	24	11	17	8	22	15
	$\left(\frac{\partial S_{MZ}}{\partial t}\right)_T$	0.32	1.65	0.99	0.53	0.14	0.34
	$S_{MZ} \left(\frac{\partial S_{MZ}}{\partial t}\right)_T^{-1}$	>60	8	21	17	>60	51
Stationary disturbances	S_{ME}	14	2	8	8	3	5
	$\left(\frac{\partial S_{ME}}{\partial t}\right)_T$	-0.25	-0.25	-0.25	-0.30	-0.10	-0.20
	$S_{ME} \left(\frac{\partial S_{ME}}{\partial t}\right)_T^{-1}$	< -60	-10	-38	-32	-46	-37

because global averages of terms of the form $\text{curl } \mathbf{B}$ (\mathbf{B} arbitrary) vanish. Enstrophy (half vorticity squared) is in this respect a more useful quantity. It was recognized first by Fjörtoft (1953) that the enstrophy budget plays an important role in determining the statistical character of a rotating fluid.

In the following we will discuss the role of $\text{curl } \mathbf{A}_H$ in the maintenance of the enstrophy of the time-mean flow. Besides brackets to denote the zonal average of s ,

$$[s] = \frac{1}{2\pi} \int_0^{2\pi} s d\lambda,$$

we will use an asterisk for the deviation from the zonal average, $s^* = s - [s]$. We then have

$$S_M = S_{MZ} + S_{ME}, \tag{7}$$

where

$$S_M = \frac{1}{2} [\bar{\zeta}^2] \\ = \text{zonally-averaged enstrophy of the time-mean flow,} \tag{8}$$

$$S_{MZ} = \frac{1}{2} [\bar{\zeta}]^2 \\ = \text{enstrophy of the zonally-averaged time-mean flow,} \tag{9}$$

$$S_{ME} = \frac{1}{2} [\bar{\zeta}^{*2}] \\ = \text{enstrophy of the stationary disturbances.} \tag{10}$$

Multiplying (1) in turn by $\bar{\zeta}$, $[\bar{\zeta}]$ and $\bar{\zeta}^*$, and taking the zonal average, one obtains for the rate of change (due to transient eddy forcing) of S_M, S_{MZ} and S_{ME} the following expressions:

$$\left(\frac{\partial S_M}{\partial t}\right)_T = [\bar{\zeta} \text{curl } \mathbf{A}_H], \tag{11}$$

$$\left(\frac{\partial S_{MZ}}{\partial t}\right)_T = [\bar{\zeta}][\text{curl } \mathbf{A}_H], \tag{12}$$

$$\left(\frac{\partial S_{ME}}{\partial t}\right)_T = [\bar{\zeta}^*(\text{curl } \mathbf{A}_H)^*]. \tag{13}$$

After averaging in the meridional and vertical directions, hemispheric and global averages of $S_M, S_{MZ}, S_{ME}, (\partial S_M/\partial t)_T, (\partial S_{MZ}/\partial t)_T$ and $(\partial S_{ME}/\partial t)_T$, and the associated e -folding times are obtained. Their numerical values are presented in Table 2. Although enstrophy is not directly related to kinetic energy, nevertheless, it is of interest to look at the corresponding values for kinetic energy, also. In analogy with the enstrophy, we define

$$K_M = K_{MZ} + K_{ME}, \tag{14}$$

where

$$K_M = \frac{1}{2} [\bar{\mathbf{V}}^2] \\ = \text{zonally-averaged kinetic energy of the time-mean flow,} \tag{15}$$

TABLE 3. As in Table 2 but for kinetic energy. Units for K_M , K_{MZ} and K_{ME} : J kg^{-1} ; for their rates of change: $10^{-6} \text{ J kg}^{-1} \text{ s}^{-1}$; and for the time scales: days.

		December–February			June–August		
		NH	SH	GL	NH	SH	GL
Time-mean flow	K_M	91	42	67	26	82	54
	$\left(\frac{\partial K_M}{\partial t}\right)_T$	13	32	22	12	28	20
	$K_M \left(\frac{\partial K_M}{\partial t}\right)_T^{-1}$	>60	15	36	27	34	31
Zonally averaged time-mean flow	K_{MZ}	79	40	60	20	79	50
	$\left(\frac{\partial K_{MZ}}{\partial t}\right)_T$	22	35	28	14	29	21
	$K_{MZ} \left(\frac{\partial K_{MZ}}{\partial t}\right)_T^{-1}$	42	13	24	19	32	27
Stationary disturbances	K_{ME}	12	2	7	6	3	4
	$\left(\frac{\partial K_{ME}}{\partial t}\right)_T$	-10	-3	-7	-2	-0	-1
	$K_{ME} \left(\frac{\partial K_{ME}}{\partial t}\right)_T^{-1}$	-14	-7	-13	-32	< -60	-44

$$K_{MZ} = \frac{1}{2}[\bar{\mathbf{V}}]^2$$

= kinetic energy of the zonally averaged time-mean flow, (16)

$$K_{ME} = \frac{1}{2}[\bar{\mathbf{V}}^{*2}]$$

= kinetic energy of the stationary disturbances. (17)

Multiplying the equation of time-mean motion (not shown here) by $\bar{\mathbf{V}}$, $[\bar{\mathbf{V}}]$ and $\bar{\mathbf{V}}^*$, and taking the zonal average one obtains for the rate of change (due to the transient eddy forcing \mathbf{A}_H) of K_M , K_{MZ} and K_{ME} , respectively,

$$\left(\frac{\partial K_M}{\partial t}\right)_T = [\bar{\mathbf{V}} \cdot \mathbf{A}_H], \quad (18)$$

$$\left(\frac{\partial K_{MZ}}{\partial t}\right)_T = [\bar{\mathbf{V}}] \cdot [\mathbf{A}_H], \quad (19)$$

$$\left(\frac{\partial K_{ME}}{\partial t}\right)_T = [\bar{\mathbf{V}}^* \cdot \mathbf{A}_H^*]. \quad (20)$$

Again, averaging in the meridional and vertical directions gives the hemispheric and global averages of K_M , K_{MZ} , K_{ME} , and $(\partial K_M/\partial t)_T$, $(\partial K_{MZ}/\partial t)_T$ and $(\partial K_{ME}/\partial t)_T$, and the associated time scales, as shown in Table 3.

Considering first the total time-mean flow one finds from Tables 2 and 3 the expected seasonal differences in S_M and K_M for the two hemispheres. It is of interest that the global average of S_M is some-

what larger in December–February (26 units) than in June–August (20 units). Taking into account the hemispheric differences in the distribution of land and ocean, this result, as well as a similar result for the kinetic energy, suggest that the atmospheric circulation would, if other effects remained equal, be stronger on a land-covered than on an ocean-covered earth. This conjecture can, of course, only be proven with the aid of general circulation simulation experiments.

When considering the rates of change of enstrophy and kinetic energy due to transient eddies one has to remember that, due to deficiencies in the station distribution (see Fig. 1), the results in the Southern Hemisphere must be less reliable than in the Northern Hemisphere. For this reason, the Northern Hemisphere values will be only discussed.

Table 2 shows that for the Northern Hemisphere as a whole, both in winter and summer, the effects of transient eddies on the enstrophy S_M are practically zero. Only a weak enstrophy input, $(\partial S_M/\partial t)_T > 0$, with a very long time scale is obtained. Table 3 shows a similar but somewhat stronger positive forcing in terms of kinetic energy. This kind of similarity between enstrophy and kinetic energy forcing is not obvious because, in principle, they could be of different sign.

Considering next the zonally averaged time-mean flow, Tables 2 and 3 show an input of both enstrophy and kinetic energy from the transient eddies; in other words, $(\partial S_{MZ}/\partial t)_T > 0$ and $(\partial K_{MZ}/\partial t)_T > 0$. The

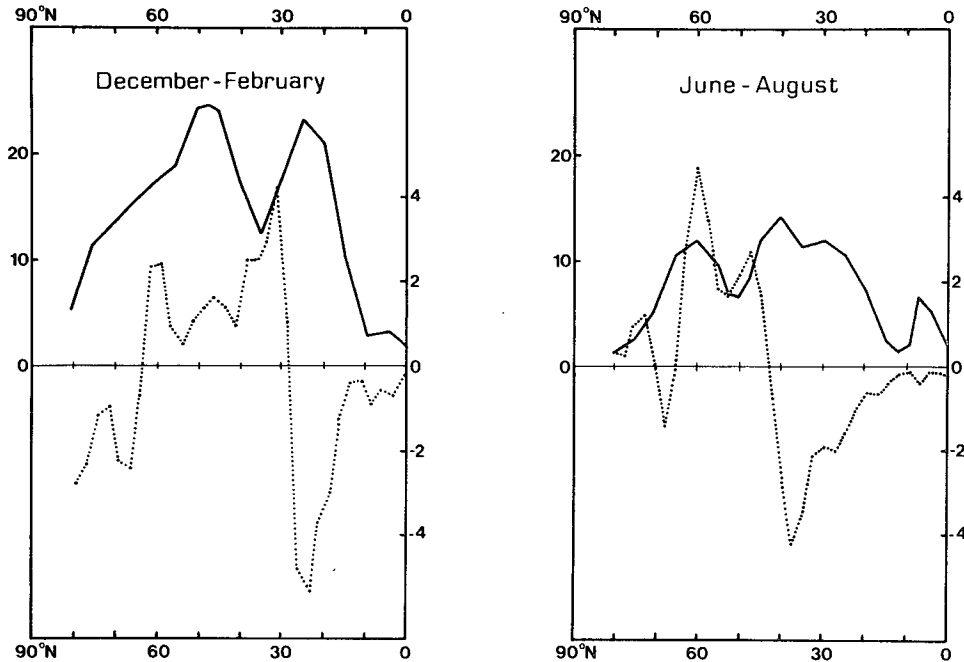


FIG. 6. Meridional profiles of the entropy in the stationary disturbances, S_{ME} (solid line), and of the transient eddy forcing, $(\partial S_{ME}/\partial t)_T$ (dashed line) averaged with respect to longitude and pressure for December-February and June-August. Units for S_{ME} 10^{-12} s^{-2} (scale on the left), for $(\partial S_{ME}/\partial t)_T$ 10^{-17} s^{-3} (scale on the right).

latter result for kinetic energy agrees with the results of earlier studies on the kinetic energy balance (e.g., Oort and Peixóto, 1974). The numerical values of the forcing terms are found to be rather small, resulting in time scales on the order of several weeks.

In case of the stationary disturbances the overall effect of the transient eddies on both entropy and kinetic energy is found to be a weak dissipative one, with a time scale of several weeks. Lau (1979) has shown that the heat fluxes associated with the transient disturbances impose a stronger dissipative effect on the horizontal temperature gradients. Thus, the total hemispheric effects of large-scale transient eddies on the stationary disturbances is definitely a dissipative one.

The values in Tables 2 and 3 refer to hemispheric and global averages. At individual latitudes, the budgets of S_{ME} and K_{ME} can be very different from these averages. This is shown for S_{ME} in Fig. 6 which gives the meridional distribution of S_{ME} and $(\partial S_{ME}/\partial t)_T$ for the Northern Hemisphere. As a result of the dipole structure of the vorticity field (see Figs. 2a and 3a) the distribution of S_{ME} exhibits two principal maxima. A more interesting feature is that the transient eddy forcing is negative in the subtropics, and positive more poleward. Thus, in terms of entropy, the quasi-permanent circulation features in middle latitudes are in part maintained by the large-scale transient eddies. This is in qualitative

agreement with the vorticity budget of the centers of action, discussed in Section 2c.

Values of S_{ME} and $(\partial S_{ME}/\partial t)_T$ averaged over the zones 0–30°N and 30–90°N are given in Table 4 for winter. The implied time scales (–8 and 17 days, respectively) are short compared with the corresponding hemispheric time scale (–67 days) in Table 2, but still somewhat longer than the dissipative time scale (~1 week) usually assigned to small-scale frictional processes. This suggests that the vorticity transfer associated with large-scale transient eddies plays a significant but not a dominant role in the maintenance of the stationary disturbances. Ultimately, they owe their existence to the forcing by mountains and longitudinal variations in diabatic heating.

TABLE 4. As in Table 2 but only for stationary disturbances in the zones 0–30°N and 30–90°N in December-February.

	0–30°N	30–90°N
S_{ME}	11	17
$\left(\frac{\partial S_{ME}}{\partial t}\right)_T$	–1.65	1.15
$S_{ME} \left(\frac{\partial S_{ME}}{\partial t}\right)_T^{-1}$	–8	17

Fig. 6 shows that the meridional distribution of $(\partial S_{ME}/\partial t)_T$ in June–August is qualitatively similar to that in winter with positive forcing in middle latitudes. The boundary between positive and negative forcing shifts from about 30°N in winter to 40°N in summer.

4. Final discussion

Our calculations show that, in terms of vorticity and enstrophy, the overall hemispheric forcing of large-scale transient eddies on the total time-mean flow is small. When the time-mean flow is decomposed into contributions from an axisymmetric component and the stationary disturbances, the transient eddy forcing is found to strengthen the axisymmetric flow and to weaken the stationary disturbances.

However, hemispherically averaged budgets often conceal important features. Thus the momentum and vorticity fluxes associated with the transient disturbances (1) show the tendency to shift the maxima of the mean westerlies poleward, and (2) provide the necessary vorticity fluxes to offset the frictional sources and sinks of vorticity at the earth's surface. For example, the transient eddies tend to maintain centers of action, such as, the North Pacific low, North Atlantic low and the Siberian high, which are the dominant stationary disturbances in the middle latitudes of the Northern Hemisphere in winter.

Because the vorticity fluxes associated with the transient waves appear to be important for the maintenance of the climatological standing waves, it is also relevant to ask how important moving weather disturbances are for the maintenance of quasi-stationary phenomena like blocking. Green (1977) has argued, that transient vorticity fluxes are indeed important. An observational study of this problem

was made by Savijärvi (1977). However, his results were not convincing, partly because of the difficulty of splitting the total local flow into mean and eddy parts in a meaningful way. Questions about the maintenance of the blocking high need further study.

Acknowledgments. The authors wish to thank Drs. I. Held, Y. Kurihara and N-C. Lau for their constructive comments on an earlier version of the manuscript, and S. Hellerman for the use of some of his ocean surface stress data. This work was performed when one of the authors (EOH) was on a Visiting Scientist appointment at the Geophysical Fluid Dynamics Program, which was supported by NOAA Grant 04-7-022-44017.

REFERENCES

- Fjørtoft, R., 1953: On the changes in the spectral distribution of kinetic energy for two-dimensional, nondivergent flow. *Tellus*, **5**, 225–230.
- Green, J. S. A., 1977: The weather during July 1976: some dynamical considerations of the drought. *Weather*, **32**, 120–126.
- Holopainen, E. O., 1978: On the dynamic forcing of the long-term mean flow by the large-scale Reynolds' stresses in the atmosphere. *J. Atmos. Sci.*, **35**, 1596–1604.
- , and A. H. Oort, 1981: Mean surface stress curl over the oceans as determined from the vorticity budget of the atmosphere. *J. Atmos. Sci.*, **38**, 262–269.
- Lau, N-C., 1979: The observed structure of tropospheric stationary waves and the local balances of vorticity and heat. *J. Atmos. Sci.*, **36**, 996–1016.
- Oort, A. H., and J. P. Peixóto, 1974: The annual cycle of the energetics of the atmosphere on a planetary scale. *J. Geophys. Res.*, **79**, 2705–2719.
- , and E. M. Rasmusson, 1971: *Atmospheric Circulation Statistics*. NOAA Prof. Pap. No. 5, 323 pp. [NTIS COM-72-50295].
- Savijärvi, H., 1977: The interaction of the monthly mean flow and large-scale transient eddies in two different circulation types. Part II: Vorticity and temperature balance. *Geophysica*, **14**, 207–229.